Boundary Element Analysis of Crack Propagation Path on Anisotropic Marble

Chien-Chung Ke[1], Shih-Meng Hsu[2], Chao-Shi Chen[3], Shu-Yeong Chi[4]

[1] Geotechnical Engineering Research Center, Sinotech Engineering Consultants, Inc. Basement No.7, Lane 26, Yat-Sen Rd., Taipei 110, Taiwan, ccke@sinotech.org.tw
[2] Geotechnical Engineering Research Center, Sinotech Engineering Consultants, Inc. Basement No.7, Lane 26, Yat-Sen Rd., Taipei 110, Taiwan, shihmeng@sinotech.org.tw
[3] Department of Resources Engineering, National Cheng Kung University, No. 1, University Rd., Tainan 701, Taiwan, chencs@ncku.edu.tw
[4] Geotechnical Engineering Research Center, Sinotech Engineering Consultants, Inc. Basement No.7, Lane 26, Yat-Sen Rd., Taipei 110, Taiwan, sychi@sinotech.org.tw

Keywords: Stress intensity factors, boundary element method, crack propagation behavior, anisotropic marble

Abstract. Rock masses in nature contain numerous discontinuities as cracks, joints, cleavages, beddings and/or even faults etc. Deformation and failure of a rock mass are greatly dependent on the presence of such geological discontinuities. In such a case, the stress intensity factors (SIFs) of crack tips, which govern the crack propagation are associated with material properties, and are strongly affected by the mechanical interaction between cracks. This paper presents the development of a unified numerical framework based on the boundary element method (BEM) for modelling crack propagation behaviour in anisotropic marble. The BEM formulation combined with the maximum circumferential stress criterion was used to predict the crack initiation angles and to simulate the crack propagation paths. To demonstrate the proposed BEM procedure to predict crack propagation in anisotropic marble, the propagation path in CSTBD specimen was numerically predicted and compared with the actual laboratory observations. Good agreement was found between the two approaches. It is therefore concluded that the proposed BEM procedure can accurately simulate the process of crack propagation for anisotropic marble.

Introduction

In 2-D crack problems, stress intensity factors are important in analysis of cracked materials. They are directly related to crack propagation criteria. The singularity of stresses near a crack tip is a challenge to numerical modelling methods, even to the BEM. Because the coincidence of the crack surfaces gives rise to a singular system of algebraic equations, the solution of cracked problem can not be obtained with the direct formulation of the BEM except for Denda [1] use a physical interpretation of Somigliana's identity to formulate it for the generalized plane strain problem. Several special methods within the scope of the BEM have been suggested for handling stress singularities, such as the Green's function method [2, 3], the sub-regional method [4-6], the displacement discontinuity method (DDM) [7-9].

The Green's function method overcomes the crack modelling problem without considering any source point along the crack boundaries. This method has the advantage of avoiding crack surface modelling and gives excellent accuracy; it is, however, restricted to very simple crack geometries for which analytical Green's function are available. The sub-regional method has the advantage of modelling cracks with any geometric shape. This method has the disadvantage of dividing the boundaries of origin region into several sub-regions, thus this method can not be easily implemented as an automatic procedure in an incremental analysis of crack extension problems. The DDM overcomes the crack modelling difficultly by replacing each pair of coincident source points on crack boundaries by a single source point [10]. Instead of using the Green's stresses and displacements from point forces, the DDM uses Green's functions corresponding to point dislocations (i.e., displacement discontinuities). This method is quite suitable for crack problems in infinite domains where there is no-crack boundary.

Recently, several single-domain BEMs have been proposed for the study of cracked media [10-22]. As a consequence, general mixed mode crack problems can be solved in a single-domain BEM formulation. The single-domain analysis can eliminate remeshing problems, which are typical of the FEM and the sub-regional BEM. The single-domain BEM has received considerable attention and has been found to be a good method for simulating crack propagation processes.
In this paper, the single-domain BEM formulation combined with the maximum circumferential stress criterion is adopted to predict the crack initiation angles and to simulate the crack propagation paths. Crack propagation in an anisotropic homogeneous plate under mixed-mode I-II loading is simulated by an incremental crack growth with a piece-wise linear discretization. A new computer program, which can automatically generate a new mesh required for analyzing the changing boundary configuration sequentially, has been developed to simulate the fracture propagation process. To demonstrate the proposed BEM procedure for predicting crack propagation in anisotropic materials, the propagation path in a CSTBD is numerically predicted and compared with the actual laboratory observations.

Theoretical Background

1. Boundary integral equations

In the BEM formulation for cracked anisotropic media, the displacement integral equation is collocated on the outer boundary only and the traction integral equation on one side of crack surface only. The displacement integral equation applied to the outer boundary results in the following form ($z^0_{k,B} \in \Gamma_B$ only, Fig. 1)

$$\begin{aligned} &C_{ij}\left(z^0_{k,B}\right)u_j\left(z^0_{k,B}\right)+\int_{\Gamma_B} T_{ij}\left(z_{k,B},z^0_{k,B}\right)u_j\left(z_{k,B}\right)d\Gamma\left(z_{k,B}\right)\\ &+\int_{\Gamma_C} T_{ij}\left(z_{k,C},z^0_{k,B}\right)\left[u_j\left(z_{k,C+}\right)-u_j\left(z_{k,C-}\right)\right]d\Gamma\left(z_{k,C}\right)\\ &=\int_{\Gamma_B} U_{ij}\left(z_{k,B},z^0_{k,B}\right)t_j\left(z_{k,B}\right)d\Gamma\left(z_{k,B}\right)\end{aligned} \tag{1}$$

where Γ_C has the same outward normal as Γ_{C+}. Here, the subscripts B and C denote the outer boundary and the crack surface, respectively.

The traction integral equation (for z^0_k being a smooth point on the crack) applied to one side of the crack surface is ($z^0_{k,C} \in \Gamma_{C+}$ only)

$$\begin{aligned} &0.5t_i\left(z^0_{k,C}\right)+n_m\left(z^0_{k,C}\right)\int_{\Gamma_B} C_{lmik}T_{ij,k}\left(z^0_{k,C},z_{k,B}\right)u_j\left(z_{k,B}\right)d\Gamma\left(z_{k,B}\right)\\ &+n_m\left(z^0_{k,C}\right)\int_{\Gamma_C} C_{lmik}T_{ij,k}\left(z^0_{k,C},z_{k,C}\right)\left[u_j\left(z_{k,C+}\right)-u_j\left(z_{k,C-}\right)\right]d\Gamma\left(z_{k,C}\right)\\ &=n_m\left(z^0_{k,C}\right)\int_{\Gamma_B} C_{lmik}U_{ij,k}\left(z^0_{k,C},z_{k,B}\right)t_i\left(z_{k,B}\right)d\Gamma\left(z_{k,B}\right)\end{aligned} \tag{2}$$

where C_{lmik} is the 4th order stiffness tensor; n_m is the unit outward normal to the contour path; the gradient tensors $T_{ij,k}$ and $U_{ij,k}$ denote differentiation with respect to z^0_k.

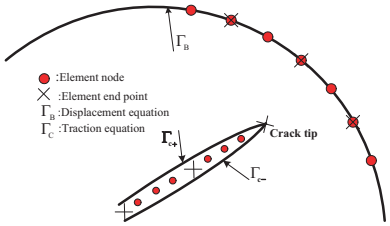

Fig. 1. Geometry of a two-dimensional cracked domain.

The Cauchy singularity in the Eq. (1) can be avoided by the rigid-body motion method. The integrand on the right-hand side of Eq. (1) has only integrable singularity, which can be resolved by the bi-cubic transformation method [23]. The hyper-singularity in the Eq. (2) is resolved by the Gauss quadrature formula, which is very similar to the traditional weighted Gauss quadrature but with a different weight. Therefore, Eqs. (1) and (2) can be solved simultaneously for the unknown displacements or tractions on the outer boundary and the unknown crack displacement differences on the crack surface.

2. Determination of SIFs

The mixed-mode SIFs for anisotropic media can be determined by using the extrapolation method of the relative crack opening displacement (COD), combined with a set of the shape functions. The relative COD is defined as [24]

$$\Delta u_i = \sum_{k=1}^{3} \phi_k \Delta u_i^k \tag{3}$$

where the subscript $i(=1, 2)$ denotes the components of the relative COD, and the superscript $k(=1, 2, 3)$ denotes the relative COD at nodes $s=-2/3$, 0, $2/3$, respectively; ϕ_k are the shape functions which can be expressed as follows.

$$\begin{aligned}
\phi_1 &= \frac{3\sqrt{3}}{8}\sqrt{s+1}[5-8(s+1)+3(s+1)^2], \\
\phi_2 &= \frac{1}{4}\sqrt{s+1}[-5+18(s+1)-9(s+1)^2], \\
\phi_3 &= \frac{3\sqrt{3}}{8\sqrt{5}}\sqrt{s+1}[1-4(s+1)+3(s+1)^2].
\end{aligned} \tag{4}$$

We assume, for simplicity, that there is a plane of material symmetry normal to the x_3-axis (or x_3-axis is a two-fold symmetry axis). Thus, the displacement u_3 does not couple with the components u_1 and u_2. For this case, the relation of the relative CODs at a distance r behind the crack-tip and the SIFs can be found as [18, 24, 25]

$$\begin{aligned}
\Delta u_1 &= 2\sqrt{\frac{2r}{\pi}}\left(H_{11}K_I + H_{12}K_{II}\right), \\
\Delta u_2 &= 2\sqrt{\frac{2r}{\pi}}\left(H_{21}K_I + H_{22}K_{II}\right).
\end{aligned} \tag{5}$$

where

$$\begin{aligned}
H_{11} &= \mathrm{Im}\left(\frac{\mu_2 P_{11} - \mu_1 P_{12}}{\mu_1 - \mu_2}\right), \quad H_{12} = \mathrm{Im}\left(\frac{P_{11} - P_{12}}{\mu_1 - \mu_2}\right), \\
H_{21} &= \mathrm{Im}\left(\frac{\mu_2 P_{21} - \mu_1 P_{22}}{\mu_1 - \mu_2}\right), \quad H_{22} = \mathrm{Im}\left(\frac{P_{21} - P_{22}}{\mu_1 - \mu_2}\right).
\end{aligned} \tag{6}$$

Substituting the Eq. (20) into Eq. (22), the SIFs K_I and K_{II} can be obtained.

3. Crack initiation and propagation

For anisotropic materials, the general form of the elastic stress field near the crack tip in the local Cartesian coordinates $x"-y"$ (shown in Fig. 2), can be expressed in terms of the two SIFs K_I and K_{II} as follows [26].

$$\sigma_{x''} = \frac{K_I}{\sqrt{2\pi r}}\mathrm{Re}\left[\frac{\mu_1\mu_2}{\mu_1-\mu_2}\left(\frac{\mu_2}{\sqrt{\cos\theta+\mu_2\sin\theta}}-\frac{\mu_1}{\sqrt{\cos\theta+\mu_1\sin\theta}}\right)\right] + \frac{K_{II}}{\sqrt{2\pi r}}\mathrm{Re}\left[\frac{1}{\mu_1-\mu_2}\left(\frac{\mu_2^2}{\sqrt{\cos\theta+\mu_2\sin\theta}}-\frac{\mu_1^2}{\sqrt{\cos\theta+\mu_1\sin\theta}}\right)\right]$$

$$\sigma_{y''} = \frac{K_I}{\sqrt{2\pi r}}\mathrm{Re}\left[\frac{1}{\mu_1-\mu_2}\left(\frac{\mu_1}{\sqrt{\cos\theta+\mu_2\sin\theta}}-\frac{\mu_2}{\sqrt{\cos\theta+\mu_1\sin\theta}}\right)\right] + \frac{K_{II}}{\sqrt{2\pi r}}\mathrm{Re}\left[\frac{1}{\mu_1-\mu_2}\left(\frac{1}{\sqrt{\cos\theta+\mu_2\sin\theta}}-\frac{1}{\sqrt{\cos\theta+\mu_1\sin\theta}}\right)\right] \tag{7}$$

$$\tau_{x''y''} = \frac{K_I}{\sqrt{2\pi r}}\mathrm{Re}\left[\frac{\mu_1\mu_2}{\mu_1-\mu_2}\left(\frac{1}{\sqrt{\cos\theta+\mu_1\sin\theta}}-\frac{1}{\sqrt{\cos\theta+\mu_2\sin\theta}}\right)\right] + \frac{K_{II}}{\sqrt{2\pi r}}\mathrm{Re}\left[\frac{1}{\mu_1-\mu_2}\left(\frac{\mu_1}{\sqrt{\cos\theta+\mu_1\sin\theta}}-\frac{\mu_2}{\sqrt{\cos\theta+\mu_2\sin\theta}}\right)\right]$$

$$\sigma_\theta = \frac{\sigma_{x''}+\sigma_{y''}}{2} - \frac{\sigma_{x''}-\sigma_{y''}}{2}\cos 2\theta - \tau_{x''y''}\sin 2\theta \tag{8}$$

$$\sigma_{r\theta} = -\frac{\sigma_{x''}-\sigma_{y''}}{2}\sin 2\theta + \sigma_{x''y''}\cos 2\theta \tag{9}$$

For the σ-criterion, the angle of crack initiation, θ_0, must satisfy

$$\frac{\partial\sigma_\theta}{\partial\theta} = 0 \quad (or \quad \tau_{r\theta} = 0) \quad and \quad \frac{\partial^2\sigma_\theta}{\partial\theta^2} < 0 \tag{10}$$

A numerical procedure is applied to find the angle θ_0 when σ_θ is maximum for known values of the material elastic constants, the anisotropic orientation angle ψ and the crack geometry.

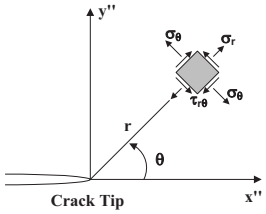

Fig. 2. Crack tip coordinate system and stress components.

The process of crack propagation in an anisotropic homogeneous material under mixed-mode I-II loading is simulated by incremental crack extension with a piece-wise linear discretization. For each incremental analysis, crack extension is conveniently modeled by a new boundary element. A computer program has been developed to automatically generate new data required for analyzing sequentially the changing boundary configuration. Based on the calculation of SIFs and crack initiation angle for each increment, the procedure of crack propagation can be simulated. The steps in the crack propagation process are summarized as follows:

1. Compute the SIFs using the proposed BEM formulation;

2. Determine the angle of crack initiation based on the maximum circumferential stress criterion;
3. Extend the crack by a linear element along the direction determined in step 2;
4. Automatically generate the new BEM mesh;
5. Repeat all the above steps until the crack is near the outer boundary.

Numerical Results

Example 1:

In order to evaluate the influence of material anisotropy on the SIFs, consider an anisotropic rectangular plate of width 2w and height 2h with a central crack inclined $45°$ to the x-axis, as shown in Fig. 3. The plate is loaded with a uniform tensile stress in the y direction. The ratios of crack length and of height to width are $a/W = 0.2$ and $h/W = 2.0$, respectively. The material is glass-epoxy with elastic properties $E = 48.26GPa$, $E' = 17.24GPa$, $\nu' = 0.29$, and $G' = 6.89GPa$ [24]. The direction of the fibers is rotated from $\psi = 0°$ to $\psi = 180°$. The outer boundary and crack surface are discretized with 32 continuous and 10 discontinuous quadratic elements, respectively. Table 1 shows the results obtained by the proposed method as well as those by Sollero and Aliabadi [27], Gandhi [28], and Chen et al. [29]. Again, an excellent agreement is obtained.

Example 2:

The proposed BEM formulation is also used to predict the initial growth of cracks in anisotropic materials. To examine the validity of our crack initiation prediction procedure, the tests of Erdogan and Sih [30] and Vallejo [31] are reproduced numerically with our BEM program.

Erdogan and Sih [30] conducted uniaxial tension test on isotropic Plexiglass sheets 229×457×4.8 mm in size containing a 50.8 mm central crack. The crack inclination angle β between the crack plane and the tensile stress is varied. Fig. 4 shows the variation of the crack initiation angle θ_0 with the crack angle β determined numerically and experimentally. A good agreement is found between the experimental results of Erdogan and Sih [30] and our numerical predictions.

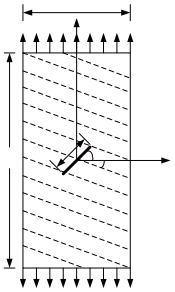

Fig. 3. An anisotropic rectangular plate with a central crack inclined 45° under uniform tensile stress σ.

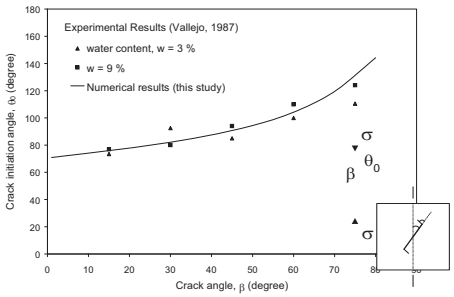

Fig. 4. Variation of crack initiation angle θ_0 with the crack angle β. Prismatic sample of kaolinite clay subjected to uniaxial compression.

Table 1. Normalized SIFs for a central slant in anisotropic rectangular plate subjected to a uniform tension ($\beta = 45°$, $a/R = 0.5$).

ψ (Deg.)	Sollero and Aliabadi (1995a)		Chen et al. (1998)		This study	
	$K_I/\sigma\sqrt{\pi a}$	$K_{II}/\sigma\sqrt{\pi a}$	$K_I/\sigma\sqrt{\pi a}$	$K_{II}/\sigma\sqrt{\pi a}$	$K_I/\sigma\sqrt{\pi a}$	$K_{II}/\sigma\sqrt{\pi a}$
0	0.517	0.506	0.519	0.504	0.524	0.514
45	0.513	0.502	0.516	0.505	0.518	0.513
90	0.515	0.510	0.537	0.532	0.533	0.527
105	0.518	0.512	0.507	0.502	0.540	0.528
120	0.526	0.513	0.520	0.508	0.541	0.526
135	0.535	0.514	0.532	0.511	0.536	0.522
180	0.517	0.506	0.519	0.504	0.524	0.514

Example 3:
The example of the anisotropic cracked Brazilian disc under mixed-mode I-II loading is carried out to investigate the validity of the current crack propagation modelling for the BEM formulation. To demonstrate the proposed BEM procedure when predicting crack propagation in the anisotropic materials under mixed-mode I-II loading, the propagation path in a CSTBD specimen is numerically predicted and compared with the actual laboratory observations. In these experiments, a crack initially inclined with respect to the applied stress is allowed to grow under concentrated diametrical loading. The Brazilian tests on CSTBD specimens with a diameter of 7.4 cm, a thickness of 1 cm, and a crack length of 2.2 cm are conducted to observe the actual propagation paths and are compared with the numerical predictions. Details of the experimental procedure can be found in the paper by Ke et al. [32]. The five elastic constants of anisotropic marble are $E = 78.302GPa$, $E' = 67.681GPa$, $\nu = 0.267$, $\nu' = 0.185$, $G = 30.735GPa$ and $G' = 25.336GPa$, respectively. The ratios of E/E' , and E/G' are 1.156 and 3.091, respectively. Since the value of $E/E' = 1.156$, this marble can be classified as a slightly anisotropic rock.

Two specimens with the material inclination angle $\psi = 45°$, defined as the B-1 and B-2 have crack angles $\beta = 0°$ and $\beta = 30°$. After Brazilian tests with cracked specimens, the paths of crack propagation for B-1 and B-2 are shown in Figs. 5 and 6, respectively. It can be observed that the crack propagates nearly perpendicular to the crack surface in the initial stage and then rapidly approaches toward the loading point. The proposed BEM procedure is also used to simulate crack propagation in the CSTBD specimens. The outer boundary and crack surface are discretized with 28 continuous and 20 discontinuous quadratic elements, respectively. Figs. 5 and 6 are the comparisons of crack propagation paths between experimental observations and numerical predictions in B-1 and B-2. Again, the proposed BEM procedure accurately simulates the crack propagation in these anisotropic specimens. According to the simulations of foregoing examples, it can be concluded that the proposed BEM is capable of predicting the crack propagation in anisotropic rocks.

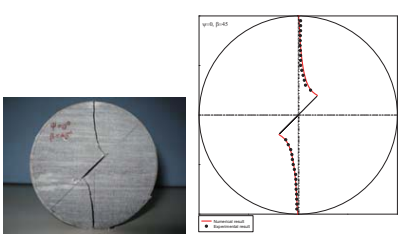

Fig. 5. Propagation of a crack at the center of a CSTBD specimen with $\psi = 0°$ and $\beta = 45°$. Comparison between experimental observations and numerical predictions for specimen B-1.

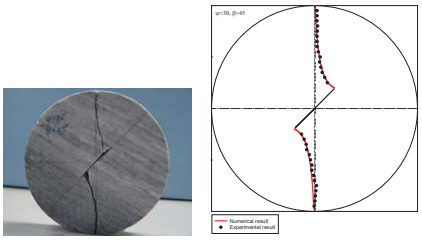

Fig. 6. Propagation of a crack at the center of a CSTBD specimen with $\psi = 30°$ and $\beta = 45°$. Comparison between experimental observations and numerical predictions for specimen B-2.

Conclusions

This paper presents the development of BEM procedure based on the maximum circumferential stress criterion for predicting the crack initiation directions and propagation paths in isotropic and anisotropic materials under mixed-mode loading. Good agreements are found between crack initiation predicted with the BEM and experimental observations reported by previous researchers of isotropic materials. Numerical simulations of crack initiation and propagation in CSTBD specimens of the anisotropic rock are also found to compare well with experimental results.

References

[1] M.Denda *Engineering Analysis with Boundary Elements*, **25**, 267-278 (2001).
[2] M.D.Snyder and T.A.Cruse *International Journal of Fracture*, **11**, 315-328 (1975).
[3] P.C.Dumir and A.K.Mehta *Computers & Structures*, **26(3)**, 431-438 (1987).

[4] G.E.Blandford, A.R.Ingraffea and J.A.Liggett *International Journal for Numerical Methods in Engineering*, **17**, 387-404 (1981).
[5] P.Sollero and M.H.Aliabadi *International Journal of Fracture*, **64**, 269-284 (1993).
[6] P.Sollero, M.H.Aliabadi and D.P.Rooke *Engineering Fracture Mechanics*, **49**, 213-224 (1994).
[7] S.L.Crouch and A.M.Starfield *Boundary Element Methods in Solid Mechanics*. George Allen and Unwin: London, 1983.
[8] B.Shen and O.Stephansson *Engineering Fracture Mechanics*, **47(2)**, 177-189 (1994).
[9] C.Scavia *Geotechnique*, **45(3)**, 447-463 (1995).
[10] A.Portela *Dual Boundary Element Analysis of Crack Growth*. Computational Mechanics: UK and USA, 1993.
[11] H.K.Hong and J.T.Chen *Journal of Engineering Mechanics*, **114**, 1028-1044 (1988).
[12] L.J.Gary, L.F.Martha and A.R.Ingraffea *International Journal for Numerical Methods in Engineering*, **29**, 1135-1158 (1990).
[13] A.Portela, M.H.Aliabadi and D.P.Rooke *International Journal for Numerical Methods in Engineering*, **33**, 1269-1287 (1992).
[14] A.Portela, M.H.Aliabadi and D.P.Rooke *Composite Structures*, **46(2)**, 237-284 (1993).
[15] P.Sollero and M.H.Aliabadi *Composite Structures*,**31**, 229-233 (1995a).
[16] P.Sollero and M.H.Aliabadi *Dual boundary element analysis of anisotropic crack problems*, *Boundary Elements XVII, Computational Mechanics* (1995b).
[17] E.Pan and B.Amadei *International Journal of Fracture*, **77**, 161-174 (1996).
[18] E.Pan *International Journal of Fracture*, **88**, 41-59 (1997).
[19] M.H.Aliabadi *International Journal of Fracture*, **86**, 91-125 (1997).
[20] J.T.Chen and H.K.Hong *Transactions of the ASME, Applied Mechanics Review*, **52(1)**, 17-33 (1999).
[21] A.P.Cisilino and M.H.Aliabadi *Engineering Fracture Mechanics*, **63**, 713-733 (1999).
[22] A.J.Wilde and M.H.Aliabadi *International Journal for Numerical and analytical Methods in Geomechanics*, **23**, 1195-1214 (1999).
[23] M.Cerrolaza and E.Alarcon *International Journal for Numerical Methods in Engineering*, **28**, 987-999 (1989).
[24] P.Sollero and M.H.Aliabadi *International Journal of Fracture*, **64**, 269-284 (1993).
[25] G.C.Sih, P.C.Paris and G.R.Irwin *International Journal of Fracture*, **3**, 189-203 (1965).
[26] G.C.Sih *Mechanics of fracture initiation and propagation: surface and volume energy density applied as failure criterion*. Kluwer (1991).
[27] P.Sollero and M.H.Aliabadi *Composite Structures*, **31**, 229-233 (1995).
[28] K.R.Gandhi *Journal of Strain Analysis*, **7(3)**, 157-162 (1972).
[29] C.S.Chen, E.Pan and B.Amadei *International Journal of Rock Mechanics and Mining Sciences*, **35(2)**, 195-218 (1998).
[30] F.Erdogan and G.C.Sih *Transactions of the ASME, Journal of Basic Engineering*, **85**, 519-527 (1963).
[31] L.E.Vallejo *Proceedings of the 28th U.S. Symposium on Rock Mechanics*, University of Arizona, Tucson (1987).
[32] C.C.Ke, C.S.Chen and C.H.Tu *Rock Mechanics and Rock Engineering*, **41(4)**, 509-538 (2008).